ON THE CHARACTERIZATION OF MU-MIMO CHANNELS

Florian Kaltenberger [1], *Laura Bernadó* [2], *Thomas Zemen* [2]

[1]Eurecom, 2229, Route des Cretes - B.P. 193, 06904 Sophia Antipolis, France
[2]ftw. Forschungszentrum Telekommunikation Wien, Donau-City-Strasse 1, 1220 Wien, Austria
Email: florian.kaltenberger@eurecom.fr, laura.bernado@ftw.at, thomas.zemen@ftw.at

ABSTRACT

In this work we study the divergence of different links in wide-band multi-user multiple-input multiple-output (MU-MIMO) channels. The divergence is measured on several levels: (i) spatial separation of the user's correlation matrices, (ii) co-linearity of the MIMO channel matrices, and (iii) correlation of large scale fading. The measurement data has been acquired using Eurecom's MIMO Openair Sounder (EMOS). The EMOS can perform real-time MIMO channel measurements synchronously over multiple users. For this work we have used an outdoor measurement with two transmit antennas and two users with two antennas each. Several measurements with different distances between users were acquired. We find that the structure of the MIMO channel matrices changes significantly with the inter-user distance. This is best captured by the co-linearity measure. The transmit and the full correlation matrix also show some dependence on the inter-user distance whereas the receive correlation matrices are independent of the inter-user distance. The shadowing correlation was found to be very low in all cases. These findings are important for MU-MIMO precoding and scheduling algorithms.

1. INTRODUCTION

In a cellular network, cooperation between users can be used to greatly increase power efficiency, reliability and throughput. Cooperation can be achieved by using the antennas of multiple users to form a virtual antenna array and by using MIMO transmission/reception techniques. The development and realistic performance assessment of such distributed MIMO systems requires measurement and characterization of the different channel links in these systems. To this end, only a limited amount of channel measurements and analysis of such distributed MIMO systems are available.

This work was supported by the European Commission in the framework of the FP7 Network of Excellence in Wireless COMmunications NEWCOM++ (contract n. 216715), the FP7 project SENDORA and Eurecom, as well as the Vienna Science and Technology Fund (WWTF) in the ftw. project COCOMINT. The Telecommunications Research Center Vienna (ftw.) is supported by the Austrian Government and the City of Vienna within the competence center program COMET.

In [1] realistic MU-MIMO channel measurements have been obtained using Eurecom's MIMO Openair Sounder (EMOS). The EMOS can perform real-time channel measurements synchronously over multiple users moving at vehicular speed. The measured channels are used to calculate the capacity of the MU-MIMO broadcast channel. One of the findings of [1] was that the performance of MU-MIMO precoding drops drastically when the users are close together in an outdoor scenario. It was further noted that this decline in performance is due to the strong correlation at the transmitter.

In this paper we investigate this phenomenon further by studying the distance of the correlation matrices with respect to the inter-user distance. Different measures to characterize the divergence of MIMO channels are available in the literature. Some of them can be applied directly on the MIMO channel matrices, while others are only applicable to correlation matrices. In this work we use the co-linearity measure applied on the channel matrices and the correlation matrix distance [2] as well as the geodesic distance [3] applied on the transmit, the receive and the full correlation matrix.

Another important phenomenon studied in this paper is the large scale shadow fading correlation. Shadowing correlation has a big impact on the performance of such cooperative communication schemes. Therefore, it is necessary to identify scenarios where shadowing correlation occurs.

An alternative correlation measure is the spectral divergence (SD) [4]. It measures the distance between strictly positive, non-normalized spectral densities. The SD was used in [5] to characterize the similarity between scattering functions of different links in a MIMO channel and in [6] to characterize the similarity between local scattering functions of a time- and frequency-selective vehicular channel. As an addition to the matrix distances we also evaluate the applicability of the SD to MU-MIMO channels.

Related work. In [7], measurements were conducted using a MEDAV-LUND channel sounder with its corresponding receiver as well as the receiver of an Elektrobit channel sounder. The two receivers are perfectly synchronized. The authors present capacity with interference results, based on the dynamic multilink measurements, as well as path-loss and delay spreads for the measured scenarios. Distributed MIMO measurements have also been described in [8]. They were

conducted with a single RUSK channel sounder using long cables between the antennas and the channel sounder. In [9] these measurements were used to characterize the spatial separation of MU-MIMO channels. The shadowing correlation between users has been studied in several papers [10–15]. However, a clear dependence of the shadowing correlation on the user distance can not be deduced.

Contribution of the paper. We show how the structure of the MIMO channel matrices changes with the inter-user distance. Further we show that the transmit and the full correlation matrix also depend on the inter-user distance whereas the receive correlation matrices are independent of the inter-user distance.

2. DESCRIPTION OF THE MEASUREMENT PLATFORM

2.1. Hardware Description

The EMOS is based on the OpenAirInterface[1] hardware/software development platform at Eurecom. The platform consists of a BS that continuously sends a signaling frame, and one or more UEs that receive the frames to estimate the channel. The BS consists of a workstation with four PCI baseband data acquisition cards, which are connected to four PLATON RF boards (see Fig. 1(a)). The RF signals are amplified and transmitted by a Powerwave 3G broadband antenna (part no. 7760.00) composed of four elements which are arranged in two cross-polarized pairs (see Fig. 1(b)). The UEs consist of a laptop computer with Eurecom's dual-RF CardBus/PCMCIA data acquisition card (see Fig. 1(c)) and two clip-on 3G Panorama Antennas (part no. TCLIP-DE3G, see Fig. 1(d)). The platform is designed for a full software-radio implementation, in the sense that all protocol layers run on the host PCs under the control of a Linux real time operation system.

2.2. Sounding Signal

The EMOS is uses an OFDM modulated sounding sequence with 256 subcarriers (out of which 160 are non-zero) and a cyclic prefix length of 64. One transmit frame is 64 OFDM symbols (2.667 ms) long and consists of a synchronization symbol (SCH), a broadcast data channel (BCH) comprising 7 OFDM symbols, a guard interval, and 48 pilot symbols used for channel estimation (see Fig. 2). The pilot symbols are taken from a pseudo-random QPSK sequence defined in the frequency domain. The subcarriers of the pilot symbols are multiplexed over the M transmit antennas to ensure orthogonality in the spatial domain. We can therefore obtain one full MIMO channel estimate for one group of M subcarriers. The BCH contains the frame number of the transmitted frame that is used for synchronization.

[1] http://www.openairinterface.org

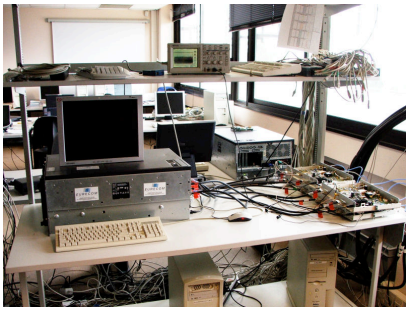

(a) Base Station with PLATON boards

(b) Power Amplifiers and Powerwave Antenna

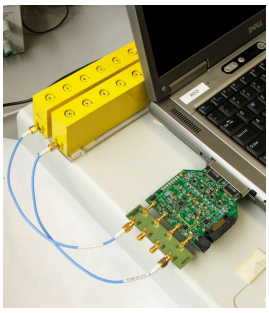

(c) Dual-RF CardBus/PCMCIA Card

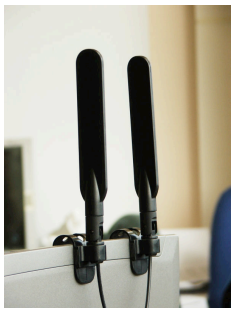

(d) Panorama Antennas

Fig. 1. EMOS base-station and user equipment [16]

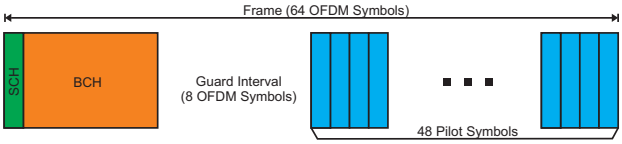

Fig. 2. Frame structure of the OFDM Sounding Sequence. The frame consists of a synchronization channel, (SCH), a broadcast channel (BCH), and several pilot symbols used for channel estimation.

2.3. Channel Estimation Procedure

Each UE first synchronizes to the BS using the SCH. It then tries to decode the data in the BCH. If the BCH can be decoded successfully, i.e., the cyclic redundancy check (CRC) is positive, then the channel estimation procedure is started. The channel estimation procedure consists of two steps. Firstly, the pilot symbols are derotated with respect to the first pilot symbol to reduce the phase-shift noise generated by the dual-RF CardBus/PCMCIA card. Secondly, the pilot symbols are averaged to increase the measurement SNR. The estimated MIMO channel is finally stored to disk. For a more detailed description of the synchronization and channel estimation procedure see [16, 17].

2.4. Multi-user Measurement Procedure

In order to conduct multi-user measurements, all the UEs need to be frame-synchronized to the BS. This is achieved by storing the frame number encoded in the BCH along with the measured channel at the UEs. This way, the measured channels can be aligned for later evaluations. The frame number is also used to synchronize the data acquisition between UEs. One measurement is 50 sec long.

3. POST PROCESSING AND PARAMETER EXTRACTION

The recorded measurement data of all users are normalized before further processing. In this section we describe the normalization, the calculation of the delay profile (PDP) and the correlation matrices. Further we define the different distance measures, i.e., the geodesic distance, the correlation matrix distance, the co-linearity and the spectral divergence.

3.1. Normalization

One measurement results in the set of MIMO matrices $\{\mathbf{H}_{k,m,q} \in \mathbb{C}^{N\times M}; k = 0,\ldots,K-1; m = 0,\ldots,N_{\mathrm{F}}-1; q = 0,\ldots,Q-1\}$, where k denotes the user index, m the snapshot index, and q the frequency (or subcarrier) index. N, M, and K are the number of receive antennas, number of transmit antennas and number of users respectively. N_{F} is the total number of snapshots per measurement after removing erroneous frames (on average $N_{\mathrm{F}} \approx 18.000$). The total number of channel estimates in the frequency domain is given by $Q = 160/M$, since there are 160 subcarriers in total and the pilots are multiplexed over the M transmit antennas. The MIMO matrices are normalized by

$$\mathbf{H}'_{k,m,q} = \mathbf{H}_{k,m,q}\sqrt{\frac{NN_{\mathrm{F}}Q}{\sum_{m,q}\|\mathbf{H}_{k,m,q}\|_F^2}} \tag{1}$$

such that $\mathbb{E}\{\|\mathbf{H}'_k\|_F^2\} = N$.

3.2. PDP Estimation

The power delay profile (PDP) is estimated by averaging the channel impulse responses of every link of the MU-MIMO channel over $A = 200$ consecutive snapshots (this corresponds to a movement of the user of apx. 4λ at the maximum speed of 5km/h). We thus introduce a new time variable $n = \lfloor m/A \rfloor$ and write

$$P_{i,j,k}[n,\tau] = \frac{1}{A}\sum_{m=An}^{A(n+1)-1}|h_{i,j,k,m,\tau}|^2, \tag{2}$$

where $h_{i,j,k,m,\tau}$ is the (i,j)-th element of the time-delay domain MIMO matrix $\mathbf{H}_{k,m,\tau}$ of user k at time m.

3.3. Correlation Matrices

The correlation matrices are also estimated by averaging over $A = 200$ consecutive snapshots and all the frequency bins. The *per-user* transmit, receive, and full correlation matrices of the MU-MIMO channel are defined as

$$\mathbf{R}^{(k)}_{\mathrm{Tx}}[n] = \frac{1}{AQ}\sum_{m=An}^{A(n+1)-1}\sum_{q=0}^{Q-1}\{\mathbf{H}^H_{k,m,q}\mathbf{H}_{k,m,q}\}, \tag{3}$$

$$\mathbf{R}^{(k)}_{\mathrm{Rx}}[n] = \frac{1}{AQ}\sum_{m=An}^{A(n+1)-1}\sum_{q=0}^{Q-1}\{\mathbf{H}_{k,m,q}\mathbf{H}^H_{k,m,q}\} \tag{4}$$

$$\mathbf{R}^{(k)}[n] = \frac{1}{AQ}\sum_{m=An}^{A(n+1)-1}\sum_{q=0}^{Q-1}\{\mathrm{vec}(\mathbf{H}_{k,m,q})\,\mathrm{vec}(\mathbf{H}_{k,m,q})^H\}. \tag{5}$$

3.4. Correlation Matrix Distances

Correlation matrices are by definition Hermitian and positive definite. The space of Hermitian and positive definite matrices forms a convex cone [3]. A natural distance measure on this cone is given by the geodesic distance

$$d_{\mathrm{Geod}}(\mathbf{R}^{(k_1)},\mathbf{R}^{(k_2)}) = \left(\sum_i |\log\lambda_i|^2\right)^{1/2}, \tag{6}$$

where λ_i are the eigenvalues of $(\mathbf{R}^{(k_1)})^{-1}\mathbf{R}^{(k_2)}$ [3]. This distance measure has been successfully used in [18] to derive a differential limited feedback scheme for MIMO communications.

Another distance for correlation matrices was introduced by [2]. It is given by

$$d_{\mathrm{Corr}}(\mathbf{R}^{(k_1)},\mathbf{R}^{(k_2)}) = \frac{\mathrm{tr}(\mathbf{R}^{(k_1)}\mathbf{R}^{(k_2)})}{\|\mathbf{R}^{(k_1)}\|_F\|\mathbf{R}^{(k_2)}\|_F}. \tag{7}$$

It becomes one if the correlation matrices are equal up to a scaling factor and zero if they differ to a maximum extent.

3.5. Channel Matrix Distance Measures

Instead of looking at the distance of correlation matrices we can also find distance measures that apply to the channel matrices directly. A simple distance measure can be derived from the zero forcing (ZF) precoder used in MU-MIMO communications [1, 19]. To keep things simple, we will use only one antenna at the receivers ($N = 1$) and denote the corresponding channel of user k with the vector $\boldsymbol{h}_k$. If the channels of two users are orthogonal, i.e., if $\boldsymbol{h}_k\boldsymbol{h}_j^H = 0$, the ZF precoder achieves the optimal sum rate. The more aligned the vectors are, i.e, the larger the scalar product $\boldsymbol{h}_k\boldsymbol{h}_j^H$, the worse the performance of ZF will be. We thus define the co-linearity measure as

$$d_{\mathrm{Colin}}(\boldsymbol{h}_{k_1},\boldsymbol{h}_{k_2}) = \frac{\boldsymbol{h}_{k_1}\boldsymbol{h}_{k_2}^H}{\|\boldsymbol{h}_{k_1}\|\|\boldsymbol{h}_{k_2}\|}. \tag{8}$$

Parameter	Value
Center Frequency	1917.6 MHz
Usefull Bandwidth	4.0625 MHz
BS Transmit Power	33 dBm
Number of Antennas at BS	2 (co-polarized)
Number of UEs	2
Number of Antennas at UE	2

Table 1. EMOS Parameters

This co-linearity measure is a special case of the co-linearity measure introduced in [9], when the number of receive antennas is one.

3.6. Shadowing Correlation

Last but not least we evaluate the correlation of the shadow fading between users. Let $s_{k,n}$ denote the shadowing component of the received signal strength in dB. This is equivalent to the digital signal strength after power control, i.e., after removing the path loss component. The shadow fading correlation coefficient between users k_1 and k_2 is defined as

$$\rho[k_1, k_2] = \frac{\mathbb{E}\{s_{k_1,n} s_{k_2,n}\}}{\sigma_{k_1}\sigma_{k_2}}, \tag{9}$$

where σ_k is the standard deviation of $s_{k,n}$ [11].

3.7. Spectral Divergence

The SD measures the distance between strictly positive, non-normalized spectral densities [4]. From our measurements we can define per each user three power spectral densities: the power delay profile, the Doppler spectral density and the angular spectral density. We define the time-dependent SD between these three time-varying power spectral divergences, where the index n denotes the time dependency. The SD between power delay profiles $P_{i,j}[n,\tau]$, between Doppler spectral densities $S_{i,j}[n,\nu]$ and between angular spectral densities $A[n,\phi,\theta]$ read

$$\gamma_n^P[k_1,k_2] = log\left(\frac{1}{(TNM)^2}\sum_{\tau,i,j}\frac{P_{i,j}^{(k_1)}[n,\tau]}{P_{i,j}^{(k_2)}[n,\tau]}\sum_{\tau,i,j}\frac{P_{i,j}^{(k_2)}[n,\tau]}{P_{i,j}^{(k_1)}[n,\tau]}\right),$$

$$\gamma_n^S[k_1,k_2] = log\left(\frac{1}{(PNM)^2}\sum_{\nu,i,j}\frac{S_{i,j}^{(k_1)}[n,\nu]}{S_{i,j}^{(k_2)}[n,\nu]}\sum_{\nu,i,j}\frac{S_{i,j}^{(k_2)}[n,\nu]}{S_{i,j}^{(k_1)}[n,\nu]}\right),$$

$$\gamma_n^A[k_1,k_2] = log\left(\frac{1}{(NM)^2}\sum_{\phi,\theta}\frac{A^{(k_1)}[n,\phi,\theta]}{A^{(k_2)}[n,\phi,\theta]}\sum_{\phi,\theta}\frac{A^{(k_2)}[n,\phi,\theta]}{A^{(k_1)}[n,\phi,\theta]}\right),$$

respectively. The user indices are k_1 and k_2, T and P denote the number of samples in the delay and Doppler domain respectively. The number of antenna elements at the receiver and transmitter side is denoted by M and N. The angle of arrival and angle of departure are ϕ and θ and ν is de discrete Doppler shift.

Fig. 3. Map of the measurement scenario. The position of the BS antenna as well as the five measurement points are indicated.

4. MEASUREMENTS AND RESULTS

4.1. Measurement Description

The Eurecom MIMO OpenAir Sounder (EMOS) has been used to conduct measurements in the vicinity of Eurecom, Sophia-Antipolis, France. In all measurements there were 2 Tx antennas and 2 UEs with two antennas each. A map of the scenario is depicted in Fig. 3. The measurement parameters are summarized in Table 1.

Two different sets of measurements were taken. In the first set, the first user was stationary and position x_1 and the second one was being pushed on a trolley from position x_1 to x_5 with a constant speed. The terminals were also equipped with GPS receivers, so that their distance can be evaluated. In the second set the first user is always at position x_1 and the second user is at position $x_i, i = 1,\ldots,5$. Positions x_1, x_2, and x_5 are LOS while positions x_3 and x_4 are behind an office building. During the measurements the users were moving only within a few wavelengths to get sufficient statistics for the evaluations.

4.2. Results

Correlation Matrix Distance. In Fig. 4 and 5 we show the geodesic distance (6) and the correlation matrix distance (7) for the transmit, the receive and the full correlation matrix over the distance between the users. The correlation matrices have been calculated as described in Equations (3)–(5) averaging over $A = 200$ frames and all frequency bins. For every such estimate, we also evaluate the distance between the users.

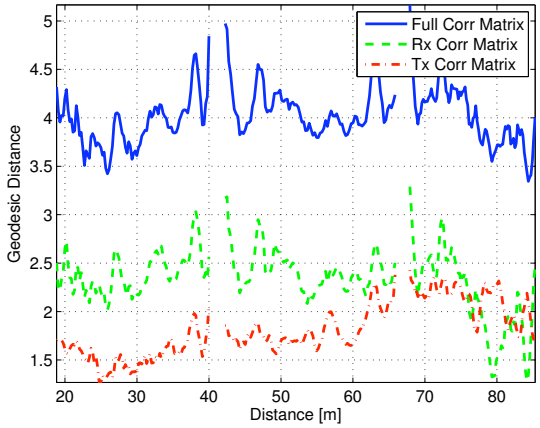

Fig. 4. Geodesic distance in dependence of the inter-user distance for the first measurement.

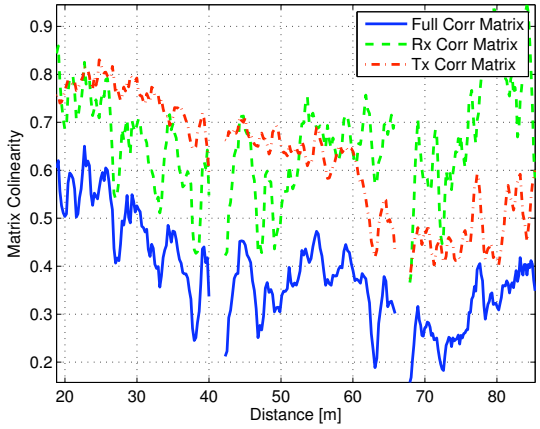

Fig. 5. Correlation matrix distance in dependence of the inter-user distance for the first measurement.

It can be seen that the geodesic distance does not show a clear dependence on the inter-user distance. The correlation matrix distance on the other hand changes significantly over distance. The full and the transmit correlation matrices are more similar when the users are close together and differ when the users are far apart. The distance between the receive correlation matrices on the other hand can not be related to the inter-user distance.

Channel Co-linearity. In Fig. 6 we plot the co-linearity between channel vectors (we use only one receive antenna). We first calculate the co-linearity for every frame m and every subcarrier q and then average over the subcarriers q. In the figure we also plot a linear function fitted to the data. A clear dependence of the co-linearity on the inter-user distance can be seen.

Shadow Fading Correlation. In Table 2 shows the shadowing correlation of second set of measurements. It can be seen that the shadowing correlation coefficient is rather low for all of the measurements.

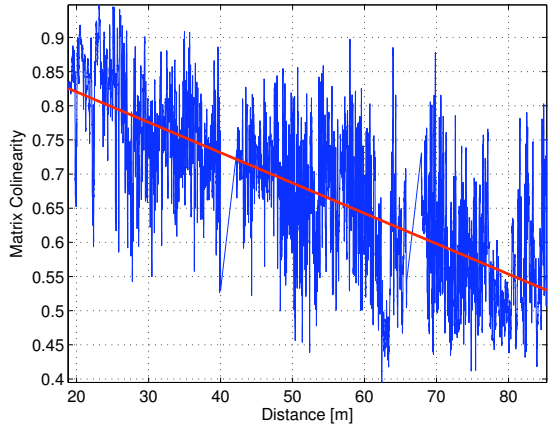

Fig. 6. Co-linearity in dependence of the inter-user distance for the first measurement. The red line is a linear function fitted to the data.

Distance [m]	1.9	15.7	32.3	53.4	76.3
Shadowing Corr.	-0.11	-0.13	-0.20	-0.08	0.01

Table 2. Shadow fading correlation in dependence of the inter-user distance for the second measurement.

Spectral Divergence. The presented results omit the SD analysis, which does not allow us to relate it to the distance between users. For the SD between power delay profiles, the value of the SD depends only on the distance from user to base station and not between users. The SD is lower when two users are at the same distance to the base station, independently of how far they are from each other. We analyse the Doppler spectral densities of two users, one of them is moving and the other remains static. We observe a constant non-zero Doppler shift for the moving user whereas the Doppler shift for the static user is zero. In this case, the SD analysis shows that the Doppler spectra between users is different, but does not present changes over distance. And finally, the analysis which could give us some meaningful results, the SD between angular spectral densities, does not have enough resultion, we only have two antenna elements at each terminal (user and base station). Because of these reasons we drop the SD analysis for this paper.

5. CONCLUSIONS

We have presented an analysis of measured MU-MIMO channels using several measures to characterize the (dis-)similarity of the channels of different users. The data was acquired us-

ing Eurecom's MU-MIMO channel sounder EMOS. The results show that the structure of the MIMO channel matrices changes significantly with the inter-user distance. This is best captured by the co-linearity measure. The transmit and the full correlation matrix also show some dependence on the inter-user distance whereas the receive correlation matrices are independent of the inter-user distance. The geodesic distance on the other hand does not show a clear dependence on the inter-user distance.

These findings are important for MU-MIMO precoding and scheduling algorithms. For example a MU-MIMO ZF precoder performs optimally if the channels of two users are orthogonal. The more aligned the channels are the worse the performance of ZF will be.

Last but not least we found that the shadowing correlation is quite low even when the nodes are quite close. This fact was also observed in other measurements [20]. However, the measurements are rather specific and thus more measurements are needed.

6. REFERENCES

[1] F. Kaltenberger, M. Kountouris, D. Gesbert, and R. Knopp, "Correlation and capacity of measured multi-user MIMO channels," in *Proc. IEEE Intl. Symposium on Personal, Indoor and Mobile Radio Communications (PIMRC)*, Cannes, France, Sep. 2008.

[2] M. Herdin, N. Czink, H. Ozcelik, and E. Bonek, "Correlation matrix distance, a meaningful measure for evaluation of non-stationary mimo channels," in *Proc. VTC 2005-Spring Vehicular Technology Conference 2005 IEEE 61st*, vol. 1, 2005, pp. 136–140.

[3] M. Talih, "Geodesic markov chains on covariance matrices," Statistical and Applied Mathematical Sciences Institute, Tech. Rep. 2007-4, mar 2007. [Online]. Available: http://www.samsi.info/TR/tr2007-04.pdf

[4] T. T. Georgiou, "Distances between power spectral densities," Tech. Rep. arXiv:math/0607026v2, Jul 2006. [Online]. Available: http://arxiv.org/abs/math.OC/0607026

[5] G. Matz, "Characterization and analysis of doubly dispersive MIMO channels," in *Asilomar Conference on Signals, Systems and Computers*, Pacific Grove, CA, USA, Oct./Nov. 2006, pp. 946–950.

[6] L. Bernadó, T. Zemen, A. Paier, G. Matz, J. Karedal, N. Czink, C. Dumard, F. Tufvesson, M. Hagenauer, A. F. Molisch, and C. F. Mecklenbräuker, "Non-WSSUS vehicular channel characterization at 5.2 GHz - coherence parameters and channel correlation function," in *Proc. XXIX General Assembly of the International Union of Radio Science (URSI)*, Chicago, Illinois, USA, Aug. 2008.

[7] J. Koivunen, P. Almers, V.-M. Kolmonen, J. Salmi, A. Richter, F. Tufvesson, P. Suvikunnas, A. F. Molisch, and P. Vainikainen, "Dynamic multi-link indoor mimo measurements at 5.3 GHz," in *Proc. 2nd European Conference on Antennas and Propagation (EuCAP 2007)*, Edinburgh, UK, Nov. 2007.

[8] N. Czink, B. Bandemer, G. V. Vilar, L. Jalloul, and A. Paulraj, "Can multi-user MIMO measurements be done using a single channel sounder?" COST 2100, Lille, France, Tech. Rep. TD(08) 621, Nov. 2008.

[9] ——, "Spatial separation of multi-user mimo channels," COST 2100, Lille, France, Tech. Rep. TD(08) 622, Nov. 2008.

[10] M. Gudmundson, "Correlation model for shadow fading in mobile radio systems," *Electronics Letters*, vol. 27, no. 23, pp. 2145–2146, 7 Nov. 1991.

[11] F. Graziosi and F. Santucci, "A general correlation model for shadow fading in mobile radio systems," *IEEE Commun. Lett.*, vol. 6, no. 3, pp. 102–104, 2002.

[12] E. Perahia, D. C. Cox, and S. Ho, "Shadow fading cross correlation between basestations," in *Vehicular Technology Conference, 2001. VTC 2001 Spring. IEEE VTS 53rd*, vol. 1, 2001, pp. 313–317.

[13] R. Wang and D. Cox, "Channel modeling for ad hoc mobile wireless networks," in *Vehicular Technology Conference, 2002. VTC Spring 2002. IEEE 55th*, vol. 1, 2002, pp. 21–25.

[14] J. Weitzen and T. J. Lowe, "Measurement of angular and distance correlation properties of log-normal shadowing at 1900 mhz and its application to design of pcs systems," *IEEE Trans. Veh. Technol.*, vol. 51, no. 2, pp. 265–273, 2002.

[15] C. Oestges, N. Czink, B. Bandemer, P. Castiglione, F. Kaltenberger, and A. Paulraj, "Experimental characterization of outdoor-to-indorr and indoor distributed channels," Universite de Louvain, Tech. Rep., 2009, in preparation.

[16] R. de Lacerda, L. S. Cardoso, R. Knopp, M. Debbah, and D. Gesbert, "EMOS platform: real-time capacity estimation of MIMO channels in the UMTS-TDD band," in *Proc. International Symposium on Wireless Communication Systems (IWCS)*, Trondheim, Norway, Oct. 2007.

[17] F. Kaltenberger, L. Bernadó, and T. Zemen, "Characterization of measured multi-user mimo channels using the spectral divergence measure," COST 2100, Lille, France, Tech. Rep. TD(08) 640, Nov. 2008.

[18] D. Sacristán-Murga, F. Kaltenberger, A. Pascual-Iserte, and A. I. Pérez-Neira, "Differential feedback in mimo communications: Performance with delay and real channel measurements," in *Workshop on Smart Antennas (WSA 2009)*, Berlin, Germany, Feb. 2009.

[19] F. Kaltenberger, M. Kountouris, L. S. Cardoso, R. Knopp, and D. Gesbert, "Capacity of linear multi-user MIMO precoding schemes with measured channel data," in *Proc. IEEE Intl. Workshop on Signal Processing Advances in Wireless Communications (SPAWC)*, Recife, Brazil, Jul. 2008.

[20] P. Kyosti, J. Meinila, L. Hentila, X. Zhao, T. Jamsa, C. Schneider, M. Narandzic, M. Milojevic, A. Hong, J. Ylitalo, V.-M. Holappa, M. Alatossava, R. Bultitude, Y. de Jong, and T. Rautiainen, "WINNER II Channel Models," European Commission, Deliverable IST-WINNER D1.1.2 ver 1.1, Sep. 2007. [Online]. Available: https://www.ist-winner.org/WINNER2-Deliverables/D1.1.2v1.1.pdf